



HAL
open science

Unexpected dimerization of a tripeptide comprising a β,γ -diamino acid

Yang Wan, Jean-Pierre Baltaze, Cyrille Kouklovsky, Emeric Miclet, Valérie Alezra

► **To cite this version:**

Yang Wan, Jean-Pierre Baltaze, Cyrille Kouklovsky, Emeric Miclet, Valérie Alezra. Unexpected dimerization of a tripeptide comprising a β,γ -diamino acid. *Journal of Peptide Science*, 2019, 25 (2), pp.e3143. 10.1002/psc.3143 . hal-03989036

HAL Id: hal-03989036

<https://hal.science/hal-03989036>

Submitted on 14 Feb 2023

HAL is a multi-disciplinary open access archive for the deposit and dissemination of scientific research documents, whether they are published or not. The documents may come from teaching and research institutions in France or abroad, or from public or private research centers.

L'archive ouverte pluridisciplinaire **HAL**, est destinée au dépôt et à la diffusion de documents scientifiques de niveau recherche, publiés ou non, émanant des établissements d'enseignement et de recherche français ou étrangers, des laboratoires publics ou privés.

Unexpected Dimerization of a Tripeptide Comprising a β,γ -Diamino Acid

Yang Wan,^{[a] [b]} Jean-Pierre Baltaze^[b] Cyrille Kouklovsky,^[b] Emeric Miclet,^[c] Valérie Alezra*^[b]

^[a] National Pharmaceutical Engineering Center for Solid Preparation in Chinese Herbal Medicine, Jiangxi University of Traditional Chinese Medicine, Nanchang 330006, PR China

^[b] Faculté des Sciences d'Orsay, Univ. Paris-Sud, Laboratoire de Méthodologie, Synthèse et Molécules Thérapeutiques, ICMMO, UMR 8182, CNRS, Université Paris-Saclay, Bât 410, 91405 Orsay, France
Email: valerie.alezra@u-psud.fr

^[c] Sorbonne Université, École normale supérieure, PSL University, CNRS, Laboratoire des biomolécules, LBM, 75005 Paris, France

Abstract: We have previously reported the synthesis of enantiopure β,γ -diamino acids and relevant short α/γ -peptide containing such building blocks. Complete NMR studies, together with molecular modeling, highlighted the ability of a β,γ -diamino acid to induce various intramolecular turns. In this paper, we describe for the first time the formation of a dimeric structure constituted by $\alpha/\gamma/\alpha$ -tripeptide and stabilized by intermolecular interactions. A structural model is proposed based on extensive NMR measurements.

Introduction

The design and construction of peptidomimetic foldamers is a challenging yet potentially highly rewarding work that contributes to the development of functional structures, biomaterials and bioactive compounds. Indeed, tremendous artificially versatile peptidic architectures based on unnatural amino acids have proved that they are potent mimics of natural folding patterns such as helices, sheets and turns [1–7]. In this domain, β -peptides have been long-investigated [8,9], γ -peptides, in contrast, have been more recently developed but are interesting as well [10–14]. The constrained forces to stabilize the three dimensional structure are including (but not limited to) hydrogen bonds, stereoelectronic interactions, local conformational control or solvophobic effects [15,16]. Nevertheless, although intermolecular interactions are important as well (for amyloid fibrils or for biologically active nanotubes [17,18] for instance), they are far less studied [19–25]. In our group, we have been dedicated on construction of structurally diverse β,γ -diamino acids [26]. When included in short peptides, they act as turn inducer to construct stable structures or optimize bioactive molecules [27–31]. In this work, we show that another tripeptide with different configuration (Figure 1) does no longer form any intramolecular hydrogen bond but induces intermolecular interaction. According to various NMR studies, specially DOSY [32], we reveal herein the dimeric structure of this new hybrid tripeptide.

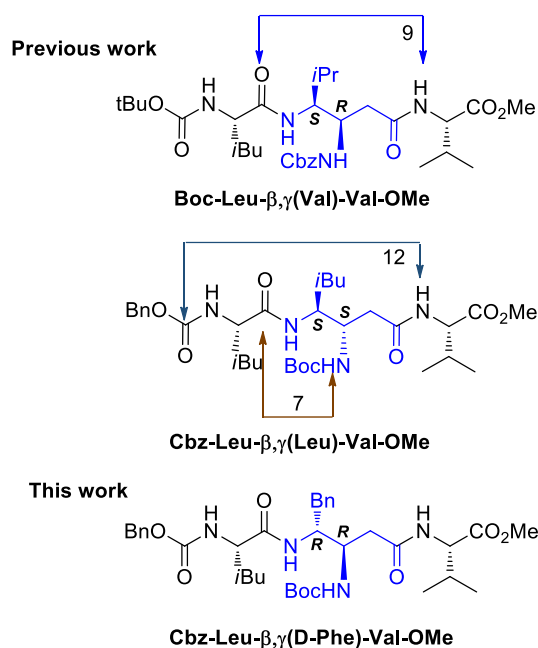
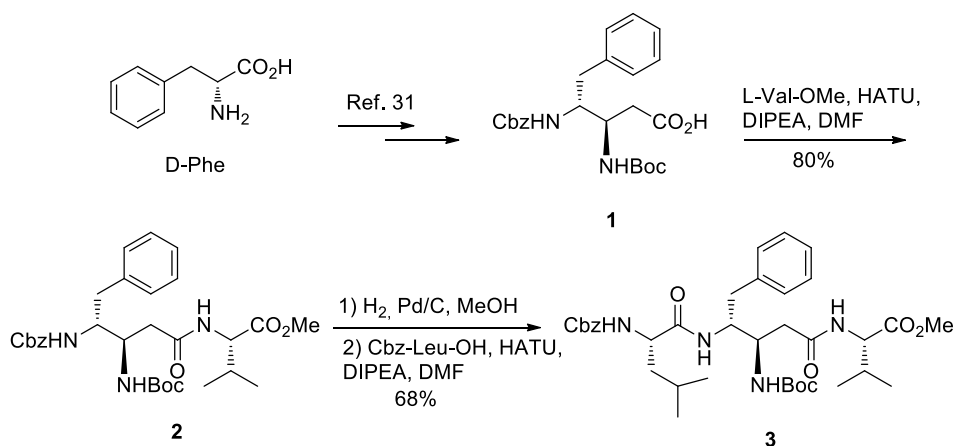


Figure 1. Structure of previous tripeptides with hydrogen bonding and of tripeptide of this work.

Results and discussion

1. Synthesis

β,γ -Diamino acid **1** was synthesized following our previously reported protocol [31]. Dipeptide **2** was synthesized through coupling compound **1** with L-Val-OMe in 80% yield. After hydrogenation in the presence of 10 wt. % Pd/C, it reacted with Cbz-Leu-OH to give rise to tripeptide **3** in 68% yield (Scheme 1).



Scheme 1. Synthesis of $\alpha/\gamma/\alpha$ -tripeptide **3**

2. Classical NMR studies

^1H NMR in CD_3OH and CDCl_3

We then embarked on detailed structural studies of $\alpha/\gamma/\alpha$ -tripeptide **3**. It is soluble in both methanol and chloroform. When ^1H NMR spectroscopy was performed in methanol- d_3 , large spectral dispersion was observed in both HN and aliphatic regions.

Extensive NMR data (NOESY, COSY, HSQC) allowed the assignment of proton and carbon resonances, but the absence of long-range NOE correlation implies that no stable folded conformation exists. When performed in CDCl₃ and at low concentration, the ¹H NMR spectrum showed a decreased spectral dispersion. However, we noticed that, in a 50 mM solution of tripeptide **3** in CDCl₃, eight HN peaks were present, corresponding to two populations interconverting in the slow exchange regime (Figure 2).

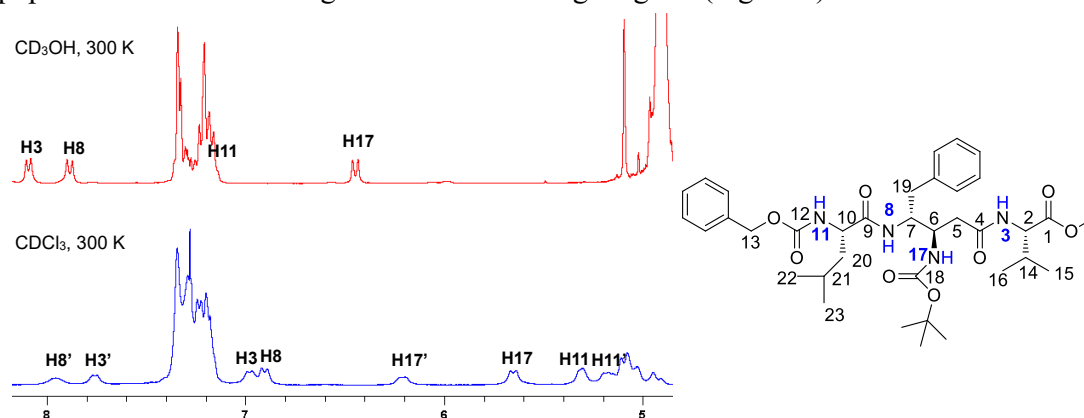


Figure 2. ¹H NMR spectra of a 50 mM solution of tripeptide **3** in CD₃OH (*upper*) and CDCl₃ (*bottom*) at 300 K (aliphatic regions were removed for clarity).

2D NMR in CDCl₃

2D NMR spectroscopies (COSY, NOESY and ¹H-¹⁵N-HSQC) were then undertaken to allow the complete proton assignment in the HN region (Figure 2, *bottom*). All 2D NMR experiments were performed using a 50 mM solution of tripeptide **3** in CDCl₃. Exchange correlations were detected in the NOESY spectrum, reflecting the dynamic equilibrium between the two populations (Figure 3, *left*). Additionally, a significant ¹⁵N chemical shift difference between the amides and the carbamate groups was found in ¹H-¹⁵N HSQC (Figure 3, *right*), which is consistent with our HN assignments. In addition to severe overlaps, aliphatic resonances were strongly broadened by the chemical exchange and were not fully assigned, except for the methyl ester and *tert*-butyl groups that displayed sharp singlets.

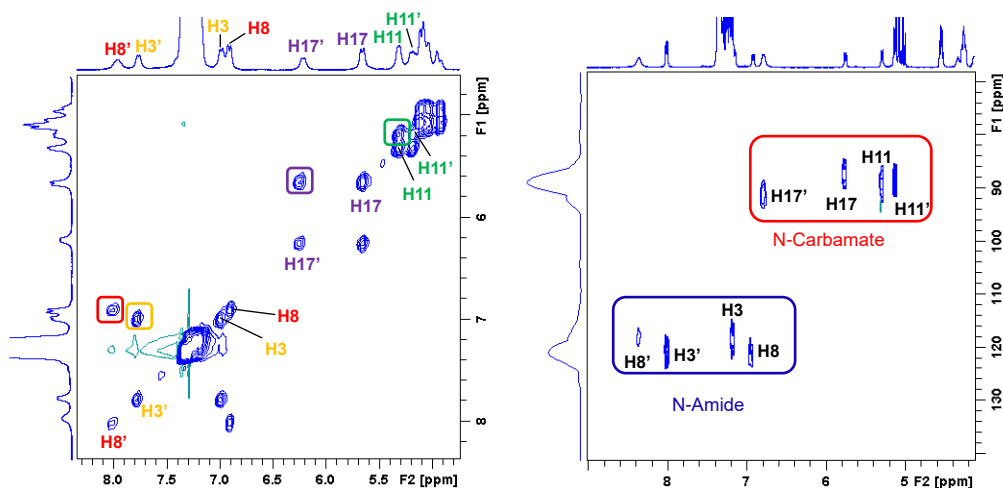


Figure 3. Exchange correlations observed in the HN-HN region of the NOESY spectrum of tripeptide **3** (360 MHz, 300 K, *left*). *N*-carbamate and *N*-amide are circled with red and blue squares respectively in the ^1H - ^{15}N HSQC spectrum of tripeptide **3** (400 MHz, 273 K, *right*).

Concentration dependence

The spectral exchange could be due to a conformational equilibrium between two monomeric states of peptide **3**. Alternatively, it could result from an oligomerization process. To gain some insights into the molecular dynamics of peptide **3**, we recorded proton spectra at different concentrations ranging from 5 mM to 100 mM in CDCl_3 (Figure 4). When the concentration was below 10 mM, a single population was identified. Meanwhile, we noticed that no HN resonance was observed at $\delta > 7$ ppm, suggesting that no intramolecular H-bond was present according to our previous work [27,29]. However, when the concentration was higher than 10 mM, a second set of proton resonances (denoted H_i') raised at significantly higher chemical shifts. These findings pointed out the formation of new species stabilized at high concentrations, presumably oligomers, which encompass peptides with well-defined structures rather than a conformational equilibrium between monomeric species [33].

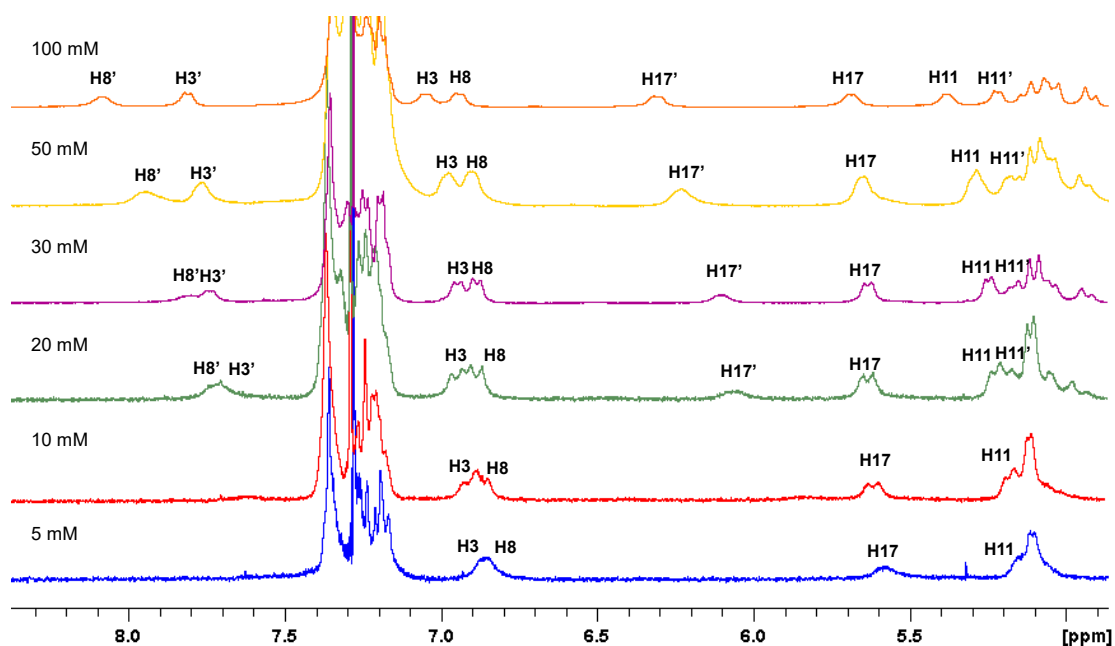


Figure 4. Variable-concentration ^1H NMR spectra of a solution of tripeptide **3** in CDCl_3 at 300 K (250 MHz). From *bottom* to *top*: increasing concentration from 5 mM to 100 mM.

Temperature dependence

Besides, the behavior of tripeptide **3** at variable temperature was investigated. ^1H NMR spectra were recorded in a 50 mM solution of tripeptide **3** in CDCl_3 for temperatures ranging from 260 K to 320 K (Figure 5), which clearly demonstrated that a low temperature favors the formation of oligomeric species. Temperature was increased and decreased showing that the observed phenomenon was reversible which excludes the possibility of a degradation. T-coefficients $\Delta\delta/\Delta T$ were calculated to discriminate H-bonded (exchange-protected) and solvent-exposed HNs (*see supporting information Table 1*). All T-coefficients were very small for the monomer (absolute value of (3.9 ± 2.6) ppb/K on average), which is consistent with the absence of intramolecular H-bond denoted previously. In contrast, much larger $|\Delta\delta/\Delta T|$ (18.7, 18.3, 12.0 ppb/K for $\text{H8}'$, $\text{H17}'$, $\text{H3}'$ respectively) were obtained for the oligomer in HN region. Such large temperature dependences prove that NH groups are initially shielded from solvent (hydrogen bonded or buried) and are transferred to exposed environments when the temperature is raised. This can be due either to dissociating aggregates or to unfolding species. [34].

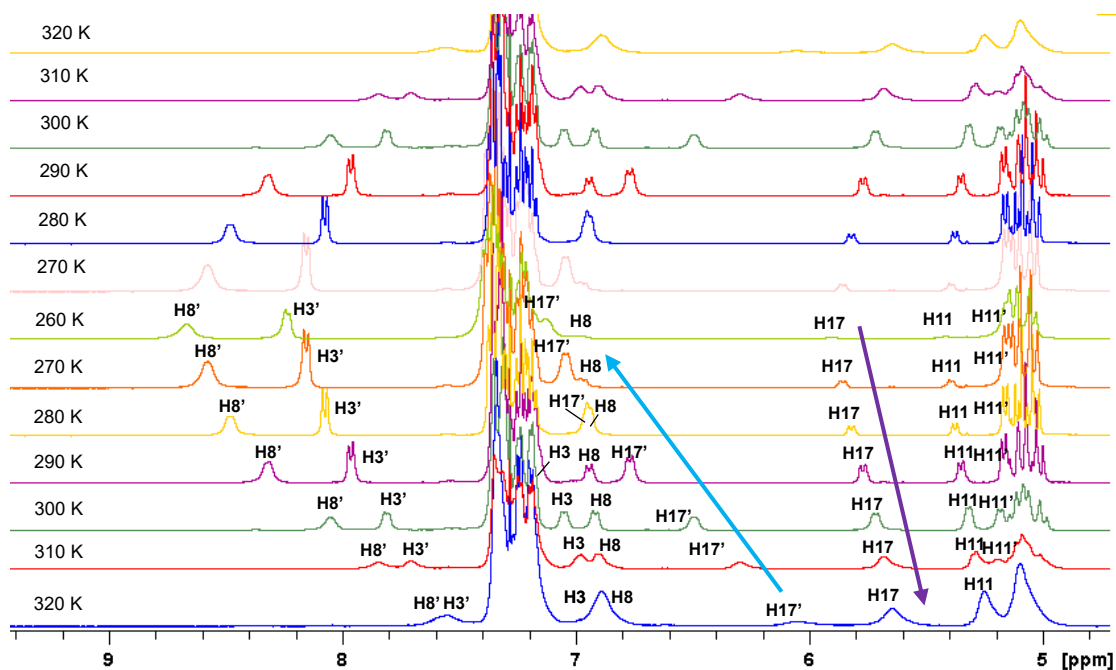


Figure 5. Variable-temperature ^1H NMR spectra in a 50 mM solution of tripeptide **3** in CDCl_3 . From bottom to top: decreasing temperature from 320 K to 260 K then increasing back to 320 K (400 MHz).

When the temperature is decreased from 320 K to 260 K, the proportion of oligomer increases (exemplified by $\text{H17}'$, blue arrow) (cf. Figure 6 and table 2 in supporting information) whereas the proportion of monomer decreases (exemplified by H17 , purple arrow). When temperature is increasing back to 320 K, the proportion of oligomer decreases whereas the proportion of monomer increases. The larger line shapes observed at high temperature are due to a faster chemical exchange between the two states which is getting closer to the intermediate regime. The coalescence temperature could not be reached in CDCl_3 .

When possible, the amounts of monomer and oligomer at each temperature have then been determined based on the integration of each amide resonance (*See supporting information Table 2*). The measured population followed a sigmoidal variation as a function of temperature. Data were fitted to the Boltzman equation using a Levenberg-Marquardt algorithm, as implemented in the Origin® software (Figure 6):

$$y(T) = \frac{A_1 - A_2}{1 + e^{(T - T_m)/\tau}} + A_2,$$

where A_1 and A_2 represent the population limits of the oligomer at low and high temperature respectively, T_m is the temperature at which half of the oligomer is dissociated and τ accounts for the temperature range of this process. The following values have been obtained for the tripeptide **3** at 50 mM in CDCl_3 :

$$A_1 = (91.2 \pm 3.1) \%$$

$$A_2 = (27.7 \pm 3.9) \%$$

$$T_m = (291.9 \pm 1.5) \text{ K}$$

$$\tau = (10.5 \pm 1.9) \text{ K}$$

According to these data, the monomeric form accounts for ~10% of the tripeptide **3** at low temperature whereas ~25% of the oligomer is still present at high temperatures. This reveals the relative stability of the oligomer in CDCl₃ although the melting temperature was ~292K.

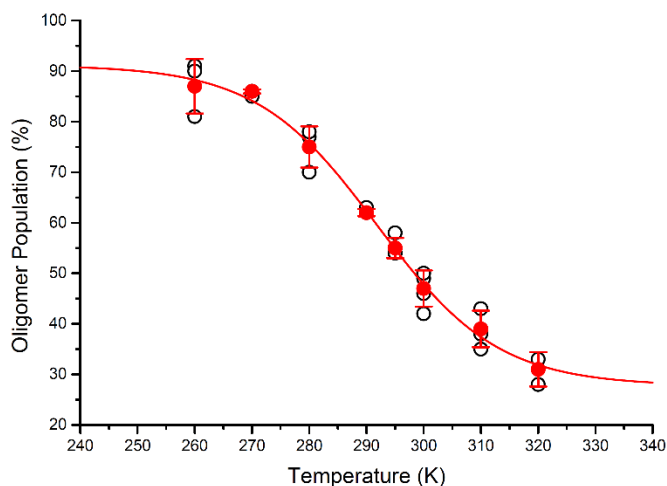


Figure 6. Sigmoidal fitting of the fractions of oligomer-**3** in a 50 mM solution of tripeptide in CDCl₃, between 260 K and 320 K. Oligomer populations were found identical when the temperature was raised or lowered.

As no intermediate oligomeric species were detected, the equilibrium between monomer and oligomer may be considered as simple two-states interconversion. Oligomer stability was assessed by performing a DMSO titration (*see supporting information*) [35]. 20 μL of DMSO-*d*₆ were successively added to a 500 μL solution (20 mM) of tripeptide **3** in CDCl₃. The number of ¹H resonances decreased significantly when 40 μL DMSO were added, which again demonstrated the existence of oligomers in CDCl₃ that are not stable in DMSO, presumably due to the disruption of intermolecular hydrogen bonds.

3. DOSY experiment and calculations

Knowing the existence of a peptide oligomer in CDCl₃, we decided to record DOSY experiments to determine the degree of oligomerization. To avoid solvent self-convection effects that interfere with the measurement of diffusion coefficients [36], we chose the 1,2-dichlorobenzene-*d*₄ (o-DCB-*d*₄) instead of CDCl₃. ¹H NMR spectrum was performed using a 5 mM solution due to the limited solubility of the tripeptide **3** in this solvent. However, the same oligomerization process was observed in o-DCB-*d*₄, since two sets of

resonances were also observed for the amide protons with chemical shifts very close to those obtained in CDCl₃ (Figure 7).

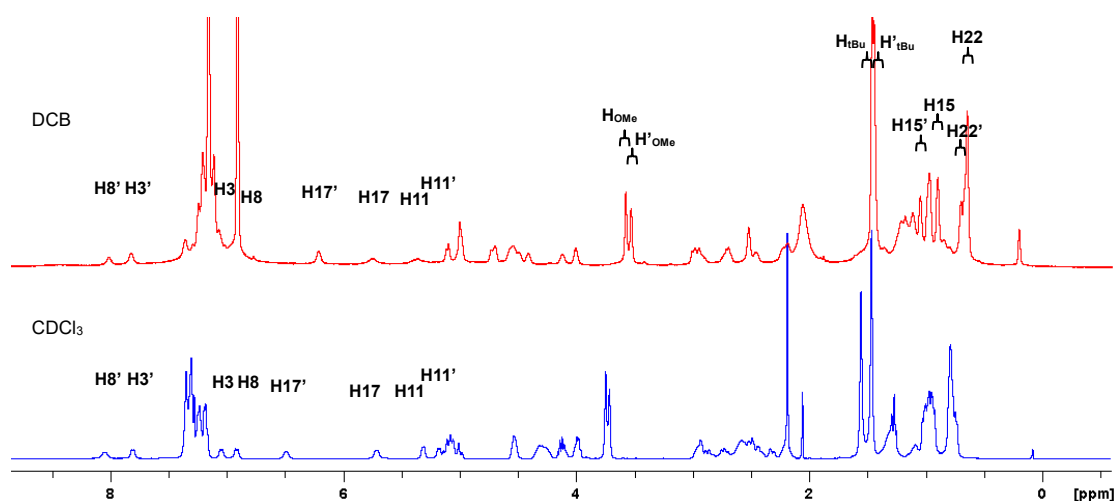


Figure 7. Comparison of ¹H NMR spectra of tripeptide **3** in DCB (5 mM, 273 K) and CDCl₃ (50 mM, 300 K). Resonances chosen for DOSY calculations were indicated by brackets.

Diffusion coefficients (D) were calculated using the following function [37]:

$$\ln I(g) = \left[-(\gamma g \delta)^2 D \left(\Delta - \frac{\delta}{3} \right) \right] + \ln(I_0)$$

where I(g) is the signal intensity measured in the DOSY experiment, as a function of the gradient strength g. I(g) also depends on the diffusion coefficient D, the gyromagnetic ratio 'γ' (rad.T⁻¹.s⁻¹) and the delays δ and Δ are fixed in the DOSY pulse sequence. The values obtained for ln I(g) were displayed as a function of g² for several resonances and then fitted with a linear curve (*see supporting information*). The diffusion coefficients are readily extracted from the slope of these curves. HN resonances were discarded from the analysis, since they are subject to chemical exchange. In addition, some aliphatic protons were also not considered due to severe resonance overlaps. Finally, we were able to measure the diffusion coefficients D with a good accuracy for four aliphatic resonances of tripeptide **3**, either in the monomeric or in the oligomeric state (Table 1). These values allowed us to calculate two averaged D with RMSD values:

$$D_{\text{oligo}} = 1.277 \times 10^{-10} \pm 0.013 \text{ m}^2/\text{s} \text{ and } D_{\text{mono}} = 1.443 \times 10^{-10} \pm 0.025 \text{ m}^2/\text{s}.$$

Table 1 1D-Diffusion coefficients of selected proton resonance

| assignment | monomer | | | | | oligomer | | | | |
|--|------------------|------------------|-----------------|-----------------|-------------|-------------------|-------------------|------------------|------------------|-------------|
| | H _{OMe} | H _{tBu} | H ₁₅ | H ₂₂ | average | H' _{OMe} | H' _{tBu} | H' ₁₅ | H' ₂₂ | average |
| δ (ppm) | 3.57 | 1.46 | 0.90 | 0.64 | | 3.53 | 1.44 | 1.05 | 0.70 | |
| Ds (10 ⁻¹⁰ m ² /s) | 1.42 | 1.42 | 1.48 | 1.45 | 1.443±0.025 | 1.26 | 1.29 | 1.29 | 1.27 | 1.277±0.013 |

The average D value obtained for the oligomer is only slightly smaller than the one measured for the monomeric tripeptide **3**, with a $D_{\text{mono}}/D_{\text{oligo}}$ ratio of 1.13. Considering spherical shapes for the monomer and the oligomer, this would result in a mass ratio $M_{\text{oligo}}/M_{\text{mono}}$ of 1.45, which falls well below the value expected for a dimer ($M_{\text{dimer}}/M_{\text{mono}} = 2$). However, compared to spherical particles, ellipsoid particles display diffusion coefficients smaller by the shape factor F [37,38]. The shape factor F corresponds to the ratio f/f_0 , where f is the friction coefficient of the molecule and f_0 the friction coefficient of a hard sphere with equivalent mass. F can be expressed as a function of the axial ratio p of the particle (see Figure 8):

$$F = (1 - p^2)^{1/2} / \{p^{2/3} \ln[1 + (1 - p^2)^{1/2}]\}, \text{ for prolate ellipsoid } (p < 1)$$

$$\text{or } F = (p^2 - 1)^{1/2} / \{p^{2/3} \tan^{-1}[(p^2 - 1)^{1/2}]\}, \text{ for oblate ellipsoid } (p > 1)$$

To gain some insights into the structure of the peptide **3** assemblies, we calculated the theoretical $F_{\text{oligo}}/F_{\text{mono}}$ ratio for oligomers increasing in size, using the experimentally determined $D_{\text{mono}}/D_{\text{oligo}}$ ratio and the following equation:

$$\frac{F_{\text{oligo}}}{F_{\text{mono}}} = \frac{D_{\text{mono}}}{D_{\text{oligo}}} \times \left(\frac{M_{\text{oligo}}}{M_{\text{mono}}}\right)^{-1/3}$$

$F_{\text{oligo}}/F_{\text{mono}}$ ratio spreads between 0.9 to 0.5 for oligomers ranging from dimer to decamer. Whatever the size of the oligomer is, the shape factor F_{oligo} should be therefore lower than the shape factor of the monomer. This means that the oligomer is more compact. It is however improbable that the monomeric tripeptide **3**, for which no defined structure has been found, possesses a high aspect ratio. With p values of 3 and 1 for the monomer and the oligomer, shape factors are equal to 1.1 and 1 respectively, which is consistent with a dimer ($F_{\text{oligo}}/F_{\text{mono}}=0.9$). For a trimer, using the measured $D_{\text{mono}}/D_{\text{oligo}}$ ratio, a value of 0.78 would be obtained for $F_{\text{oligo}}/F_{\text{mono}}$. This would imply a p axial ratio and not aspect ratio greater than 6 for the monomer which is unlikely. These measurements of diffusion coefficient are then consistent with the formation of a dimer at high concentration and low temperature.

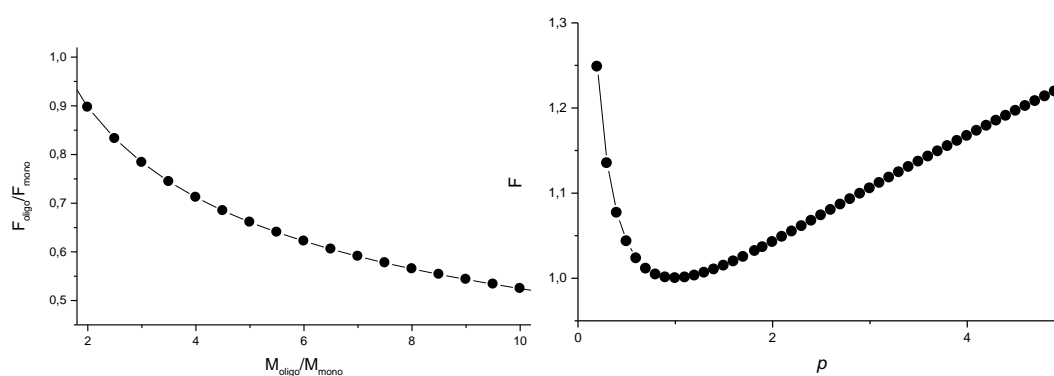


Figure 8. left panel : F values derived from the experimentally determined D ratio and calculated for oligomers increasing in size (from a dimer to a decamer). Right panel: F as a function of the axial ratio p of the particle.

4. Further conformational analysis and hypothesis on dimeric structure

The further step investigation was carried out at 240K with using a 200mM sample in CDCl_3 . At this temperature and using such a high concentration, we observed solely the dimer. Extensive NMR studies allowed the complete assignment of proton and carbon resonances. Impressively, several ROE correlations between long-range protons were extracted from the ROESY spectrum (Figure 9). As we have confirmed the absence of intramolecular H-bond, the observed ROEs resulted from intermolecular interactions.

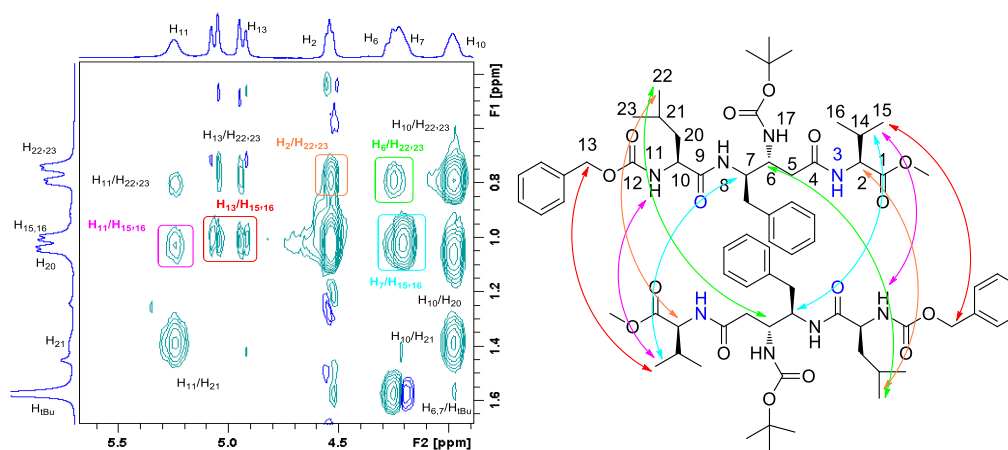


Figure 9. ROEs observed in ROESY spectrum of a 200 mM solution of tripeptide **3** in CDCl_3 (400 MHz, 240 K).

Indeed, exclusively four HN resonances were observed for dimeric structure, which means that the dimeric structure is symmetric. Considering the distances network deduced from the ROESY spectrum, the two monomers presumably adopt an *anti*-parallel orientation with the Cbz group close to the valine of the other molecule. This arrangement is in good agreement with a lower shape factor for the dimer compared to the monomer [38]. By taking into account the amide protons displaying high T-coefficients, we hence propose that the dimer is stabilized by six intermolecular hydrogen bonds (Figure 10) involving the HN from L-Val residue and both NH from the β,γ -diamino acid residue (T-coefficients are respectively 13.0, 19.2 and 18.0 ppb/K). Such a role of the central β,γ -diamino acid in the peptide dimerization would also explain why the $^3J_{\text{H6-H17}}$ measured for the dimer (9.3 Hz) significantly differs from the value obtained for the monomer ($^3J_{\text{H6-H17}}=8.6$ Hz).

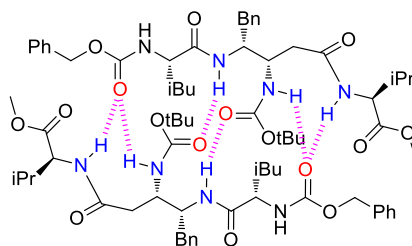


Figure 10. Proposed arrangement for the dimeric structure.

Conclusions

In this work, we observed that a short hybrid peptide sequence incorporating a β,γ -amino acid is able to self-assemble into oligomer in solution. After a detailed structural investigation by NMR, in particular by DOSY and ROESY NMR, we have thus highlighted an *anti*-parallel dimeric structure stabilized by six intermolecular H-bonds. Such dimeric structures are very original and very stable due to the increased hydrogen bonds donor and acceptor present in a β,γ -diamino acid residue. Further studies are under investigation in our lab to use this template for antimicrobial peptide and amyloid inhibitors design.

Acknowledgment: We thank the CSC (China Scholarship Council, doctoral grant for Y.W.) for financial support.

Compliance with ethical standards

This research does not involve any human or animal participant

Conflict of interest: The authors declare that they have no conflict of interest.

Supporting information: Procedures, characterization data, ^1H and ^{13}C NMR spectra of the peptides, variable temperature and concentration ^1H NMR spectra, NMR data tables, DMSO titration, DOSY spectrum and fittings.

References

- Hill DJ, Mio MJ, Prince RB, Hughes TS, Moore JS. A Field Guide to Foldamers. *Chem. Rev.* 2001; **101**: 3893–4012; DOI:10.1021/cr990120t.
- Gellman SH. Foldamers: A Manifesto. *Acc. Chem. Res.* 1998; **31**: 173–180; DOI:10.1021/ar960298r.
- Guichard G, Huc I. Synthetic Foldamers. *Chem. Commun.* 2011; **47**: 5933–5941; DOI:10.1039/C1CC11137J.
- Seebach D, Gardiner J. β -Peptidic Peptidomimetics. *Acc. Chem. Res.* 2008; **41**: 1366–1375; DOI:10.1021/ar700263g.
- Liskamp RMJ, Rijkers DTS, Kruijtz JAW, Kemmink J. Peptides and Proteins as a Continuing Exciting Source of Inspiration for Peptidomimetics. *ChemBioChem* 2011; **12**: 1626–1653; DOI:10.1002/cbic.201000717.

- 6 Goodman CM, Choi S, Shandler S, DeGrado WF. Foldamers as Versatile Frameworks for the Design and Evolution of Function. *Nat. Chem. Biol.* 2007; **3**: 252–262; DOI:10.1038/nchembio876.
- 7 Vasudev PG, Chatterjee S, Shamala N, Balaram P. Structural Chemistry of Peptides Containing Backbone Expanded Amino Acid Residues: Conformational Features of β , γ , and Hybrid Peptides. *Chem. Rev.* 2011; **111**: 657–687; DOI:10.1021/cr100100x.
- 8 Laursen JS, Engel-Andreasen J, Olsen CA. β -Peptoid Foldamers at Last. *Acc. Chem. Res.* 2015; **48**: 2696–2704; DOI:10.1021/acs.accounts.5b00257.
- 9 Pils LKA, Reiser O. α/β -Peptide Foldamers: State of the Art. *Amino Acids* 2011; **41**: 709–718; DOI:10.1007/s00726-011-0894-2.
- 10 Bouillère F, Thétiot-Laurent S, Kouklovsky C, Alezra V. Foldamers Containing γ -Amino Acid Residues or Their Analogues: Structural Features and Applications. *Amino Acids* 2011; **41**: 687–707; DOI:10.1007/s00726-011-0893-3.
- 11 Fisher BF, Gellman SH. Impact of γ -Amino Acid Residue Preorganization on α/γ -Peptide Foldamer Helicity in Aqueous Solution. *J. Am. Chem. Soc.* 2016; **138**: 10766–10769; DOI:10.1021/jacs.6b06177.
- 12 Mathieu L, Legrand B, Deng C, Vezenkov L, Wenger E, Didierjean C, Amblard M, Averlant-Petit M-C, Masurier N, Lisowski V, Martinez J, Maillard LT. Helical Oligomers of Thiazole-Based γ -Amino Acids: Synthesis and Structural Studies. *Angew. Chem. Int. Ed.* 2013; **52**: 6006–6010; DOI:10.1002/anie.201302106.
- 13 Vasudev PG, Ananda K, Chatterjee S, Aravinda S, Shamala N, Balaram P. Hybrid Peptide Design. Hydrogen Bonded Conformations in Peptides Containing the Stereochemically Constrained γ -Amino Acid Residue, Gabapentin. *J. Am. Chem. Soc.* 2007; **129**: 4039–4048; DOI:10.1021/ja068910p.
- 14 Awada H, Grison CM, Charnay-Pouget F, Baltaze J-P, Brisset F, Guillot R, Robin S, Hachem A, Jaber N, Naoufal D, Yazbeck O, Aitken DJ. Conformational Effects through Hydrogen Bonding in a Constrained γ -Peptide Template: From Intraresidue Seven-Membered Rings to a Gel-Forming Sheet Structure. *J. Org. Chem.* 2017; **82**: 4819–4828; DOI:10.1021/acs.joc.7b00494.
- 15 Zhao Y, Moore JS. Foldamers Based on Solvophobic Effects. In *Foldamers*, Hecht S, Huc I (eds). Wiley-VCH Verlag GmbH & Co. KGaA, 2007; 75–108.
- 16 Huc I, Cuccia L. Foldamers Based on Local Conformational Preferences. In *Foldamers*, Hecht S, Huc I (eds). Wiley-VCH Verlag GmbH & Co. KGaA, 2007; 1–33.
- 17 Valéry C, Pouget E, Pandit A, Verbavatz J-M, Bordes L, Boisdé I, Cherif-Cheikh R, Artzner F, Paternostre M. Molecular Origin of the Self-Assembly of Lanreotide into Nanotubes: A Mutational Approach. *Biophys. J.* 2008; **94**: 1782–1795; DOI:10.1529/biophysj.107.108175.
- 18 Wang F, Carabino JM, Vergara CM. Insulin Glargine: A Systematic Review of a Long-Acting Insulin Analogue. *Clin. Ther.* 2003; **25**: 1541–1577; DOI:10.1016/S0149-2918(03)80156-X.
- 19 Yoo SH, Lee H-S. Foldectures: 3D Molecular Architectures from Self-Assembly of Peptide Foldamers. *Acc. Chem. Res.* 2017; **50**: 832–841; DOI:10.1021/acs.accounts.6b00545.

- 20 Montalvo GL, Zhang Y, Young TM, Costanzo MJ, Freeman KB, Wang J, Clements DJ, Magavern E, Kavash RW, Scott RW, Liu D, DeGrado WF. De Novo Design of Self-Assembling Foldamers That Inhibit Heparin–Protein Interactions. *ACS Chem. Biol.* 2014; **9**: 967–975; DOI:10.1021/cb500026x.
- 21 Yashima E, Ousaka N, Taura D, Shimomura K, Ikai T, Maeda K. Supramolecular Helical Systems: Helical Assemblies of Small Molecules, Foldamers, and Polymers with Chiral Amplification and Their Functions. *Chem. Rev.* 2016; **116**: 13752–13990; DOI:10.1021/acs.chemrev.6b00354.
- 22 Zhang Y, Cao R, Shen J, Detchou CSF, Zhong Y, Wang H, Zou S, Huang Q, Lian C, Wang Q, Zhu J, Gong B. Hydrogen-Bonded Duplexes with Lengthened Linkers. *Org. Lett.* 2018; **20**: 1555–1558; DOI:10.1021/acs.orglett.8b00283.
- 23 Collie GW, Pulka-Ziach K, Lombardo CM, Fremaux J, Rosu F, Decossas M, Mauran L, Lambert O, Gabelica V, Mackereth CD, Guichard G. Shaping Quaternary Assemblies of Water-Soluble Non-Peptide Helical Foldamers by Sequence Manipulation. *Nat. Chem.* 2015; **7**: 871–878; DOI:10.1038/nchem.2353.
- 24 Reiriz C, Amorín M, García-Fandiño R, Castedo L, Granja JR. α,γ -Cyclic Peptide Ensembles with a Hydroxylated Cavity. *Org. Biomol. Chem.* 2009; **7**: 4358–4361; DOI:10.1039/B911247M.
- 25 Luder K, Kulkarni K, Lee HW, Widdop RE, Borgo MPD, Aguilar M-I. Decorated Self-Assembling B3-Triptide Foldamers Form Cell Adhesive Scaffolds. *Chem. Commun.* 2016; **52**: 4549–4552; DOI:10.1039/C6CC00247A.
- 26 Hoang CT, Bouillère F, Johannesen S, Zulauf A, Panel C, Pouilhès A, Gori D, Alezra V, Kouklovsky C. Amino Acid Homologation by the Blaise Reaction: A New Entry into Nitrogen Heterocycles. *J. Org. Chem.* 2009; **74**: 4177–4187; DOI:10.1021/jo900324d.
- 27 Thétiot-Laurent S, Bouillère F, Baltaze J-P, Brisset F, Feytens D, Kouklovsky C, Miclet E, Alezra V. Original β,γ -Diamino Acid as an Inducer of a γ -Turn Mimic in Short Peptides. *Org. Biomol. Chem.* 2012; **10**: 9660–9663; DOI:10.1039/C2OB26828K.
- 28 Bouillère F, Feytens D, Gori D, Guillot R, Kouklovsky C, Miclet E, Alezra V. Constrained α/γ -Peptides: A New Stable Extended Structure in Solution without Any Hydrogen Bond and Characterized by a Four-Fold Symmetry. *Chem. Commun.* 2012; **48**: 1982–1984; DOI:10.1039/C2CC16852A.
- 29 Stanovych A, Guillot R, Kouklovsky C, Miclet E, Alezra V. β,γ -Diamino Acid: An Original Building Block for Hybrid α/γ -Peptide Synthesis with Extra Hydrogen Bond Donating Group. *Amino Acids* 2014; **46**: 2753–2757; DOI:10.1007/s00726-014-1831-y.
- 30 Wan Y, Auberger N, Thétiot-Laurent S, Bouillère F, Zulauf A, He J, Courtiol-Legourd S, Guillot R, Kouklovsky C, Cote des Combes S, Pacaud C, Devillers I, Alezra V. Constrained Cyclic β,γ -Diamino Acids from Glutamic Acid: Synthesis of Both Diastereomers and Unexpected Kinetic Resolution. *Eur. J. Org. Chem.* 2018; **2018**: 329–340; DOI:10.1002/ejoc.201701477.
- 31 Wan Y, Stanovych A, Gori D, Zirah S, Kouklovsky C, Alezra V. β,γ -Diamino Acids as Building Blocks for New Analogues of Gramicidin S: Synthesis and Biological

- Activity. *Eur. J. Med. Chem.* 2018; **149**: 122–128; DOI:10.1016/j.ejmech.2018.02.053.
- 32 Schaeffer G, Fuhr O, Fenske D, Lehn J-M. Self-Assembly of a Highly Organized, Hexameric Supramolecular Architecture: Formation, Structure and Properties. *Chem. – Eur. J.* 2014; **20**: 179–186; DOI:10.1002/chem.201303186.
- 33 Adler-Abramovich L, Gazit E. The Physical Properties of Supramolecular Peptide Assemblies: From Building Block Association to Technological Applications. *Chem. Soc. Rev.* 2014; **43**: 6881–6893; DOI:10.1039/C4CS00164H.
- 34 Stevens ES, Sugawara N, Bonora GM, Toniolo C. Conformational Analysis of Linear Peptides. 3. Temperature Dependence of NH Chemical Shifts in Chloroform. *J. Am. Chem. Soc.* 1980; **102**: 7048–7050; DOI:10.1021/ja00543a025.
- 35 Halab L, Lubell WD. Use of Steric Interactions To Control Peptide Turn Geometry. Synthesis of Type VI β -Turn Mimics with 5-Tert-Butylproline. *J. Org. Chem.* 1999; **64**: 3312–3321; DOI:10.1021/jo990294a.
- 36 Jerschow A, Müller N. Suppression of Convection Artifacts in Stimulated-Echo Diffusion Experiments. Double-Stimulated-Echo Experiments. *J. Magn. Reson.* 1997; **125**: 372–375; DOI:10.1006/jmre.1997.1123.
- 37 Chou JJ, Baber JL, Bax A. Characterization of Phospholipid Mixed Micelles by Translational Diffusion. *J. Biomol. NMR* 2004; **29**: 299–308; DOI:10.1023/B:JNMR.0000032560.43738.6a.
- 38 Yao S, Howlett GJ, Norton RS. Peptide Self-Association in Aqueous Trifluoroethanol Monitored by Pulsed Field Gradient NMR Diffusion Measurements. *J. Biomol. NMR* 2000; **16**: 109–119; DOI:10.1023/A:1008382624724.